ISSN 1990-7931, Russian Journal of Physical Chemistry B, 2018, Vol. 12, No. 4, pp. 620–631. © Pleiades Publishing, Ltd., 2018.
Original Russian Text © S.O. Adamson, V.V. Kuverova, G.K. Ozerov, G.V. Golubkov, Sh.Sh. Nabiev, M.G. Golubkov, 2018, published in Khimicheskaya Fizika, 2018, Vol. 37, No. 7, pp. 3–15.

ELEMENTARY PHYSICOCHEMICAL PROCESSES

Ab Initio Calculation of the Lowest Singlet and Triplet Excited States of the N_2 Molecule

S. O. Adamson[a, b], V. V. Kuverova[c], G. K. Ozerov[d], G. V. Golubkov[a, e, *], Sh. Sh. Nabiev[e], and M. G. Golubkov[a]

[a] *Semenov Institute of Chemical Physics, Russian Academy of Sciences, Moscow, 119991 Russia*
[b] *Moscow State University, Moscow, 119991 Russia*
[c] *Center for Chemical Physics of Atmosphere, Moscow, 117977 Russia*
[d] *Skolkovo Institute of Science and Technology, Moscow, 121205 Russia*
[e] *National Research Center "Kurchatov Institute," Moscow, 123182 Russia*
**e-mail: golubkov@chph.ras.ru*

Received March 2, 2018

Abstract—Ab initio calculations of the adiabatic potential curves and matrix elements of radial nonadiabatic coupling of the N_2 molecule for the states related to dissociation limits I–V were performed. The most important spectral characteristics of the adiabatic states agreed well with the available experimental and theoretical data. The diabatic states were constructed. The diabatic quantum defects and radial matrix elements of the configuration interaction of the dissociative and Rydberg configurations whose states converge to the ground state $X^2\Sigma_g^+$ and the first electronically excited state $A^2\Pi_u$ of the N_2^+ ion were calculated. The possibility of using the results for calculating the cross sections and rate constants of dissociative recombination and associative ionization within the framework of the multichannel quantum defect theory was discussed.

Keywords: molecular nitrogen, Rydberg states, quantum defect, ab initio calculations
DOI: 10.1134/S1990793118040024

1. INTRODUCTION

The dissociative recombination $N_2^+ + e \rightarrow N + N$ is one of the most important reactions that take place in the ionospheres of the Earth, Mars, and other planets of the solar system. The mechanism of this reaction involves the formation of nitrogen molecules in the metastable excited state due to the electron capture followed by their decay. The reaction rate and product yield depend on several factors, the most important of which are the lifetime (width) of the metastable state of N_2 and the characteristics of the dissociative electronic states, i.e., the states whose repulsive branches lie in the region between the classic turning points of the lowest states of the N_2^+ ion [1].

A correct description of the dissociative recombination of the N_2^+ ion requires the knowledge of the characteristics of dissociative states, which can be obtained from the spectral data or ab initio calculations of the highly excited electronic states of the N_2 molecule. The first method can be used only for evaluating the partial cross sections of dissociative recombination because only the states of $^{1,3}\Sigma_u^+$ and $^{1,3}\Pi_u$ symmetry were studied in detail for N_2 molecule [2]. A brief review of experimental studies covering the period of time from publication of the monograph [3] to the present time is found in [2]. Ab initio calculations of the excited states of the N_2 molecule were also performed and reviewed in detail in [2]. However, not all electronic states of interest were included in the ab initio calculations. The results of calculations were in satisfactory agreement [2].

Thus, restricting ourselves only to the dissociative recombination of the N_2^+ ion in the $X^2\Sigma_g^+$ ground state (v = 0–3), we state that the goal of this study is ab initio calculation of the potential curves and matrix elements of nonadiabatic coupling for the states that correlate with dissociation limits I–V, including the lower Rydberg states with the moments $l \leq 3$ from the series that converge to the $X^2\Sigma_g^+$ ground state and the nearest $A^2\Pi_u$ excited state of the N_2^+ ion.

2. CALCULATION PROCEDURE

The calculations of the potential curves and matrix elements of the nonadiabatic interaction of the lowest states of the N_2 molecule and N_2^+ ion were performed

by the configuration interaction method with a set of initial configurations (CMRCI) [4]. For the nitrogen atom, the [7*s*6*p*4*d*3*f*] basis of atomic orbitals (AOs) was taken, which was constructed by complementing the [3*s*2*p*1*d*1*f*] basis of natural atomic orbitals [5] with diffuse functions of *s*–*f* types (ζ_s = 0.33, 0.1, 0.03, 0.01; ζ_p = 0.5, 0.15 , 0.045, 0.0125, ζ_d = 0.33, 0.11, 0.033, ζ_f = 0.66, 0.24). As molecular orbitals (MOs), we used the natural orbitals of the multiconfiguration self-consistent field (SCF) method with averaging over the ground states of N_2 and N_2^+ and with the active space including the 2, 3σ and 1π MOs that correlate with the 2*s*2*p* AO in the dissociative limit. To form a set of initial configurations in the CMRCI method, a selection scheme was used, which was tested earlier in calculations of the NO molecule [6]. The configuration functions of the state with weights >0.005 constructed on MOs from a complete active space including the 2, $3\sigma_{u,\,g}$ and $1\pi_{u,\,g}$ correlating with the 2*s*2*p* AO and $4\sigma_g^+4\sigma_u^+$ Rydberg MOs were chosen in the CMRCI model space. To calculate the matrix elements of the radial nonadiabatic coupling, we used the finite difference method; the differentiation step was set at 0.002 a. u.

3. RESULTS AND DISCUSSION

The key element of the ab initio analysis of the results is the construction of a system of criteria that allows to compare the results of independent studies and makes it possible to evaluate the accuracy of calculations. In recent theoretical investigations devoted to the excited states of molecular nitrogen, the accuracy was evaluated by comparing the equilibrium internuclear distances R_e and the binding energies E_e of the adiabatic states with the available experimental data [1, 2, 7]. As an additional criterion of accuracy, the values of the quantum defect function taken at an equilibrium internuclear distance were used. This system of criteria, however, has a significant disadvantage: if the ab initio calculations do not use the full configuration interaction approximation, a systematic error in the binding energy appears because of the unbalanced description of the states of the neutral molecule and its ion.

3.1. Valence and Rydberg States of the N_2 Molecule

The adiabatic potential curves were calculated for 42 singlet and triplet states of $^{1,3}\Sigma_{g,u}^{\pm}$, $^{1,3}\Pi_{g,u}$, $^{1,3}\Delta_{g,u}$, $^{1,3}\Phi_{g,u}$, and $^{1,3}\Gamma_{g,u}$ symmetry, whose E_e and R_e values are presented in Table 1. The energy was measured from the $X^2\Sigma_g^+$ ground state of the N_2^+ ion. A comparison of the data of Table 1 shows that the results are in good agreement both with the experimental [3, 8–11] and theoretical data [1, 2, 7, 12] only in the case when the absolute value of the binding energy exceeds 2.5 eV. However, the energy difference between the ground state of the nitrogen molecule and its ion proved 0.16 eV lower than the experimental value 15.59 eV. In this case, our R_e values differ from the experimental values by no more than 0.005 Å. In the energy range $|E_e| < 2.5$ eV, the spectrum becomes more complex because along with the valence states, a large number of Rydberg states appear whose identification (assignment) is a nontrivial problem.

Figure 1 shows the differences between the experimental E_e^0 and calculated $(E_e)_{\text{calc}}$ binding energies. The calculation performed in the present study and corrected for the systematic error agrees better with the experimental data than other calculations. The maximum deviation of our values $\Delta E_e = E_e^0 - (E_e)_{\text{calc}}$, as in [7], does not exceed 0.5 eV. In other studies, it ranges from 0.7 [2] to 1.1 eV [1].

3.2. Diabatic Potential Curves of the N_2 Molecule

For processes involving diatomic molecules such as dissociative recombination (DR) or associative ionization (AI), it is often necessary to use the diabatic states, i.e., to consider isolated electronic configurations. For this purpose, it is convenient to use the diabatization method [6]. It is based on solving the variational problem of minimizing the matrix norm of the derivatives of wave functions of Rydberg and valence configurations. The method allows to efficiently calculate the main molecular characteristics (terms, quantum defects, nonadiabatic couplings) used in the multichannel quantum defect (MQD) theory for calculating the cross sections of DR and AI.

As a result, the dependences of the diabatic potential curves of the Rydberg and valence states of the N_2 molecule on the interatomic distance R were obtained. The results of calculation for the even and odd singlet and triplet diabatic states of the nitrogen molecule are shown in Fig. 2. As in Table 1, the energy is measured relative to the ground state of the ion $N_2^+(X^2\Sigma_g^+)$. In the right part of Figs. 2a–2d, the dissociative limits—the energies of dissociated atoms—are indicated.

3.3. Quantum Defects

The dependences of the adiabatic quantum defects on the internuclear distance $\mu_{nl\lambda}(R)$ were obtained from the data on the potential curves of the dependences $U_{\text{ion}}(R)$ of the ionic term $X^2\Sigma_g^+$ and Rydberg terms $U_{nl\lambda}(R)$ belonging to different Rydberg ($nl\lambda$) series. The $\mu_{nl\lambda}(R)$ dependence was calculated by the equation

$$\mu_{nl\lambda}(R) = n - [2(U_{\text{ion}}(R) - U_{nl\lambda}(R))]^{-1/2}, \qquad (1)$$

Table 1. Binding energies E_e (eV) and equilibrium internuclear distances R_e (Å) of the valence and Rydberg states of the N_2 molecule

States	This work		Experimental data			Results of other calculations		
	E_e	R_e	E_e	R_e	Ref.	E_e	R_e	Ref.
$X\,^2\Sigma_g^+$	0.000	1.125	0.000	1.116	[3]	0.000	1.125	[2]
$^3\Sigma_u^-(3d\pi_g)$	−0.239	1.178	–	–	–	−0.237	1.183	[2]
$^3\Delta_u(3d\pi_g)$	−0.269	1.178	–	–	–	−0.296	1.197	[2]
$3\,^3\Sigma_g^-$	−0.662	1.455	–	–	–	−0.456	1.518	[2]
$4\,^3\Delta_g$	−0.980	1.844	–	–	–	−1.195 −1.277	1.692 1.736	[1] [2]
$2\,^1\Pi_g$	−0.992	1.952	–	–	–	−0.893	1.886	[2]
$3\,^3\Delta_g$	−0.994	1.848	–	–	–	–	–	–
$c_5'^1\Sigma_u^+(5p\sigma_u)$	−1.060	1.124	−1.217	–	[9]	−1.241	1.136	[2]
$^3\Delta_u(4f\delta_u)$	−1.089	1.123	–	–	–	−0.861	1.125	[2]
$2\,^3\Delta_g$	−1.103	2.762	–	–	–	–	–	–
$2\,^3\Sigma_g^+$	−1.123	1.829	–	–	–	–	–	–
$4\,^3\Pi_u$	−1.155	1.492	–	–	–	–	–	–
$x\,^1\Sigma_g^-(3p\pi_u)$	−1.304	1.174	−1.526	1.173	[3]	−1.539	1.179	[2]
$^3\Sigma_g^-(3p\pi_u)$	−1.310	1.174	–	–	–	−1.349	1.181	[2]
$2\,^3\Sigma_g^-$	−1.322	1.943	–	–	–	−1.438 −1.375	1.729 1.821	[2] [7]
$y\,^1\Pi_g(3p\sigma_u)$	−1.328	1.175	−1.418	1.177	[3]	−1.253	1.175	[2]
$k\,^1\Pi_g(3d\pi_g)$	−1.330	1.128	−1.480	1.109	[3]	−1.465	1.128	[2]
$^3\Pi_g(3d\pi_g)$	−1.342	1.120	–	–	–	−1.494	1.124	[2]
$z\,^1\Delta_g(3p\pi_u)$	−1.342	1.174	−1.278	1.169	[3]	−1.331	1.155	[2]
$1\,^1\Delta_g$	−1.352	1.744	–	–	–	−1.504	1.732	[2]
$^3\Delta_g(3p\pi_u)$	−1.364	1.176	–	–	–	−1.486	1.196	[2]
$3\,^3\Pi_u$	−1.369	1.359	–	–	–	–	–	–
$^3\Sigma_g^+(3p\pi_u)$	−1.402	1.176	–	–	–	−1.482	1.189	[2]
$2\,^1\Sigma_g^+$	−1.450	2.328	–	–	–	−0.959	1.700	[2]
$d_3\,^1\Sigma_g^+(3d\sigma_g)$	−1.466	1.121	−1.699	–	[10]	−1.633	1.125	[2]
$^3\Sigma_g^+(4s\sigma_g)$	−1.488	1.125	–	–	–	−1.680	1.129	[2]

Table 1. (Contd.)

States	This work		Experimental data			Results of other calculations		
	E_e	R_e	E_e	R_e	Ref.	E_e	R_e	Ref.
$b'^1\Sigma_u^+$	−1.988	1.737	−2.634	1.444	[3]	−2.794 −2.780	1.499 1.463	[1] [2]
$o_3{}^1\Pi_u(3s\sigma_g)$	−2.123	1.151	−2.464	1.178	[3]	−2.182	1.170	[2]
$H^3\Phi_u$	−2.123	1.485	−2.483	1.488	[3]	−2.534 −2.358 −2.210	1.506 1.512 1.499	[1] [2] [7]
$F^3\Pi_u(3s\sigma_g)$	−2.184	1.183	−2.555	1.176	[11]	−2.254	1.168	[2]
$2^3\Pi_u$	−2.335	2.834	–	–	–	–	–	–
$c_3{}^1\Pi_u(3p\pi_u)$	−2.427	1.120	-2.637	1.116	[3]	−2.488	1.140	[2]
$G^3\Pi_u(3p\pi_u)$	−2.431	1.124	−2.696	1.113	[11]	−2.660	1.127	[2]
$c_4'{}^1\Sigma_u^+(3p\sigma_u)$	−2.460	1.125	−2.635	–	[9]	−2.628	1.127	[2]
$D^3\Sigma_u^+(3p\sigma_u)$	−2.515	1.124	−2.603	1.108	[3]	−2.724	1.124	[2]
$1^1\Gamma_g$	−2.571	1.727	–	–	–	−2.765 −2.821 −3.100	1.636 1.609 1.600	[2] [7] [12]
$b^1\Pi_u$	−2.769	1.330	−2.984	1.284	[3]	−3.158 −3.200	1.381 1.340	[1] [2]
$a''^1\Sigma_g^+(3s\sigma_g)$, inner	−3.109	1.122	−3.190	1.122	[3]	−3.165 −3.698	1.128 1.114	[2] [7]
$C'^3\Pi_u$	−3.187	1.522	−3.396	1.514	[3]	−3.698 −3.755 −3.286	1.535 1.534 1.527	[1] [2] [7]
$1^3\Sigma_g^-$	−3.240	1.704	–	–	–	−3.659 −3.467	1.631 1.619	[2] [7]
$E^3\Sigma_g^+(3s\sigma_g)$	−3.303	1.123	−3.705	1.117	[3]	−3.575 −3.700	1.127 1.127	[2] [7]
$1^3\Sigma_g^+$	−3.450	2.818	–	–	–	–	–	–
$2^3\Sigma_u^+$	−3.524	2.883	–	–	–	–	–	–
$a''^1\Sigma_g^+$, outer	−4.056	1.549	–	–	–	−4.570 −4.553 −4.367	1.574 1.572 1.557	[1] [2] [7]
$C^3\Pi_u$	−4.173	1.159	−4.495 −4.539	– 1.149	[8] [3]	−4.583 −4.703 −4.401	1.160 1.162 1.154	[1] [2] [7]
$G^3\Delta_g$	−4.419	1.670	−4.692	1.611	[3]	−4.608 −4.876 −4.466	1.618 1.637 1.618	[1] [2] [7]

Table 1. (Contd.)

States	This work		Experimental data			Results of other calculations		
	E_e	R_e	E_e	R_e	Ref.	E_e	R_e	Ref.
$w^1\Delta_u$	−6.468	1.266	−6.651	1.268	[3]	−7.763 −6.786 −6.470	1.280 1.282 1.295	[1] [2] [7]
$a^1\Pi_g$	−6.817	1.228	−7.000	1.220	[3]	−7.043 −7.088 −6.915	1.226 1.235 1.223	[1] [2] [7]
$a'^1\Sigma_u^-$	−6.915	1.273	−7.140	1.276	[3]	−7.274 −7.031	1.292 1.278	[2] [7]
$B'^3\Sigma_u^-$	−7.192	1.282	−7.373	1.278	[3]	−7.667 −7.349	1.292 1.283	[2] [7]
$W^3\Delta_u$	−8.000	1.282	−8.175	1.300	[3]	−8.147 −8.499 −8.243	1.285 1.293 1.283	[1] [2] [7]
$B^3\Pi_g$	−8.001	1.222	−8.198	1.213	[3]	−8.242 −8.494 −8.106	1.218 1.227 1.220	[1] [2] [7]
$A^3\Sigma_u^+$	−9.222	1.291	−9.336	1.287	[3]	−9.460 −9.946 −9.392	1.291 1.310 1.292	[1] [2] [7]
$X^1\Sigma_g^+$	−15.432	1.104	−15.590	1.098	[3]	−15.997 −15.590	1.107 1.104	[2] [7]

where n is the principal quantum number, l and λ are the orbital moment of the Rydberg electron and its projection on the axis of the molecule. Table 2 lists the values of the adiabatic quantum defects $\mu_{nl\lambda}$ at an equilibrium position R_e for the series of states that converge to the ground state $X^2\Sigma_g^+$ and first electronically excited state $A^2\Pi_u$ of the N_2^+ ion. Table 2 also gives the data of [2, 13].

It is worthwhile to note the unusual behavior of quantum defects for the $^3\Sigma_g^-(3p\pi_u)$, $x^1\Sigma_g^-(3p\pi_u)$, and $^3\Sigma_u^-(3d\pi_g)$ states belonging to the Rydberg series that converge to the $A^2\Pi_u$ state of the ion. In contrast to our assumptions, the quantum defects slightly increase for the $^3\Sigma_g^-(3p\pi_u)$ and $x^1\Sigma_g^-(3p\pi_u)$ states and abruptly decrease for the $^3\Sigma_u^-(3d\pi_g)$ state.

The calculations of the cross sections and rate constants of DR [14–16] and AI [6, 17] in the framework of the integral variant of the MQD theory use the dependences of the diabatic quantum defects $\mu_{nl\lambda}^d(R)$ included in the expression for the reaction t matrix. The calculations generally use the linear interpolation:

$$\mu_{nl\lambda}^d(R) = \mu_{nl\lambda}^d(R_e^+) + \left.\frac{d\mu_{nl\lambda}^d(R)}{dR}\right|_{R_e^+}(R - R_e^+), \qquad (2)$$

where R_e^+ is the equilibrium position of the ion nuclei. Table 3 lists the calculated values of the diabatic quantum defects and their derivatives taken at an equilibrium position for different series of the Rydberg states of the N_2 molecule, which converge to the ground $X^2\Sigma_g^+$ and first electronically excited $A^2\Pi_u$ states of the N_2^+ ion.

3.4. Configuration Interaction

In terms of the MQD theory, the complete Hamiltonian of the system is generally represented in the atomic system of units ($\hbar = m_e = e = 1$) as [18]

$$\mathbf{H} = \mathbf{H}_0 + \mathbf{V}, \qquad (3)$$

$$\mathbf{H}_0 = -\frac{1}{2}\boldsymbol{\Delta}_r - \frac{1}{r} + \mathbf{H}_q, \qquad (4)$$

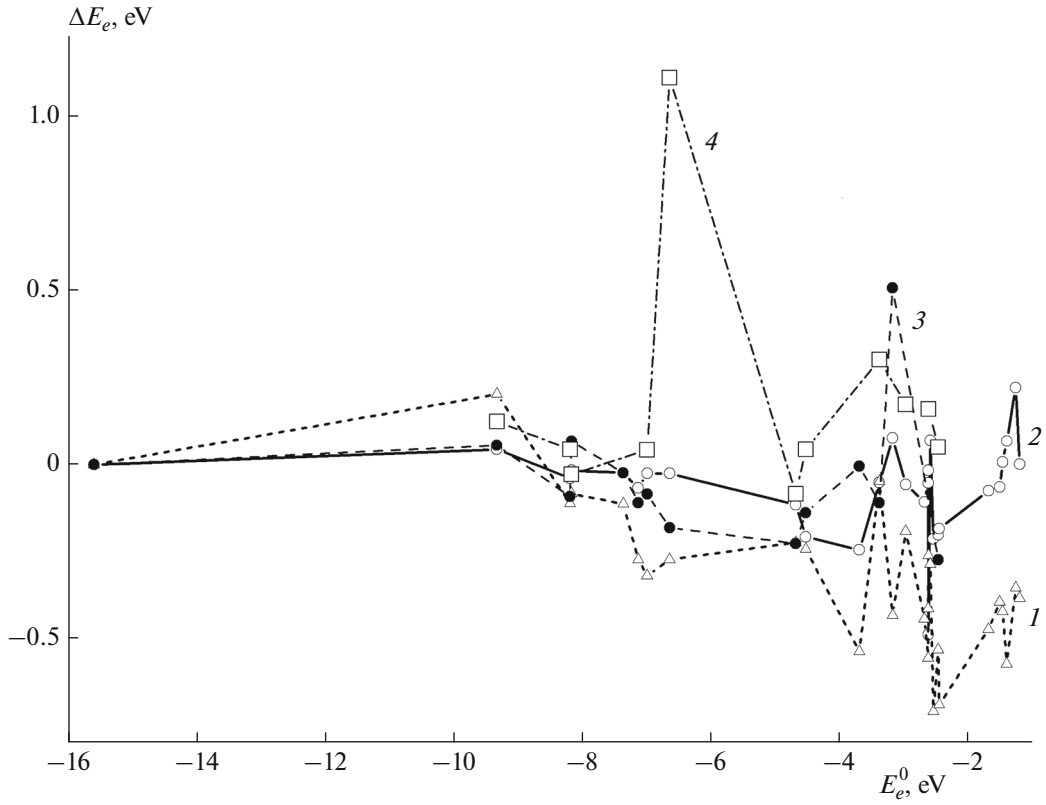

Fig. 1. Comparison of the experimental E_e^0 and calculated $(E_e)_{\text{calc}}$ binding energies $\Delta E_e = E_e^0 - (E_e)_{\text{calc}}$: the data of (*1*) [2], (*2*) our calculation, (*3*) [7], and (*4*) [1].

where $-(1/2)\mathbf{\Delta}_r$ is the kinetic energy operator of a weakly bound electron; $\mathbf{r}$ is its coordinate relative to the center of mass of the positively charged N_2^+ molecular ion; and $\mathbf{H}_q$ is the Hamiltonian of the molecular ion, which depends on the set of coordinates of inner electrons $\{\mathbf{x}\}$. The index $q = \{v, N\}$ specifies the set of vibrational (v) and rotational (N) quantum numbers of the ion. The zero Hamiltonian $\mathbf{H}_0$ is chosen such that all interactions be included in the dissociative configurations N + N*, while in the $e^- + N_2^+$ scattering channel, only the Coulomb part of interaction $V^{\text{C}} = -1/r$ should be included. Then in complete Hamiltonian (3), the operator $\mathbf{V} = \mathbf{V}^{\text{nC}} + \mathbf{V}^{\text{CI}}$ includes the non-Coulomb part of electron interaction with the ion core $\mathbf{V}^{\text{nC}}$ and the configuration interaction $\mathbf{V}^{\text{CI}}$ that binds $e^- + N_2^+$ and N + N * configurations denoted by the indices q and β. The corresponding wave functions have the form

$$|q\rangle = \sqrt{\pi}\varphi_v(\mathbf{r})\varphi_+(\mathbf{x})\chi_v(R), \quad (5)$$

$$|\beta\rangle = \sqrt{\pi}\varphi_\beta(\mathbf{r})\varphi'_+(\mathbf{x})\chi_\beta(R), \quad (6)$$

where $\varphi_v(\mathbf{r})$ and $\varphi_\beta(\mathbf{r})$ are the single-electron wave functions of these configurations, $\varphi_+(\mathbf{x})$ and $\varphi'_+(\mathbf{x})$ are the electron functions of ion residues, $\{\mathbf{x}\}$ is the set of coordinates of inner electrons, $\chi_v(R)$ is the vibrational wave function of the N_2^+ ion, and $\chi_\beta(R)$ is the nuclear wave function of the dissociative configuration. The electronic functions $|\varphi_v(\mathbf{r})\varphi_+(\mathbf{x})\rangle$ are simple two-configuration wave functions of the ground state of the ion complemented with the corresponding Rydberg orbital. The wave functions $|q\rangle$ and $|\beta\rangle$ were normalized on the energy scale as

$$\langle q(E)|q(E')\rangle = \langle\beta(E)|\beta(E')\rangle = \pi\delta(E - E'). \quad (7)$$

At the distances r between the electron and the ion core of the order of atomic distances ($r \sim a_0$, where a_0 is the radius of the first Bohr orbit) they describe the fast electron and the slow nuclear subsystem; i.e., they are adiabatic. The matrix elements of the configuration bond $\langle q|V^{\text{CI}}|\beta\rangle$ describe the configuration interaction of the $e^- + N_2^+$ and N + N * states.

Figure 3 presents the matrix elements of interaction $V_{q\beta}^{\text{CI}}(R)$ of the dissociative and Rydberg configurations,

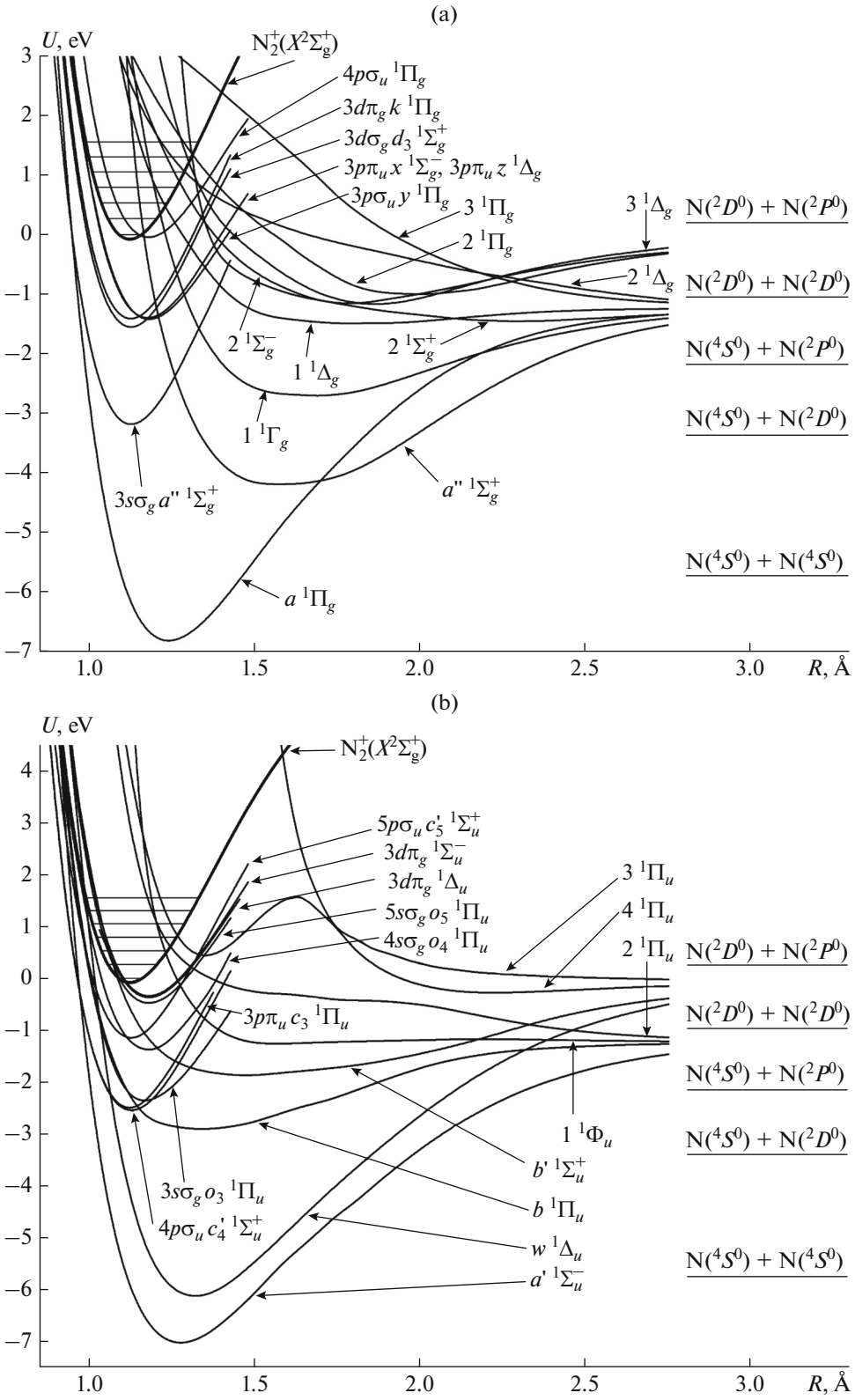

Fig. 2. Diabatic potential curves of the Rydberg and valence states of the N_2 molecule: (a) even singlet states, (b) odd singlet states, (c) even triplet states, and (d) odd triplet states.

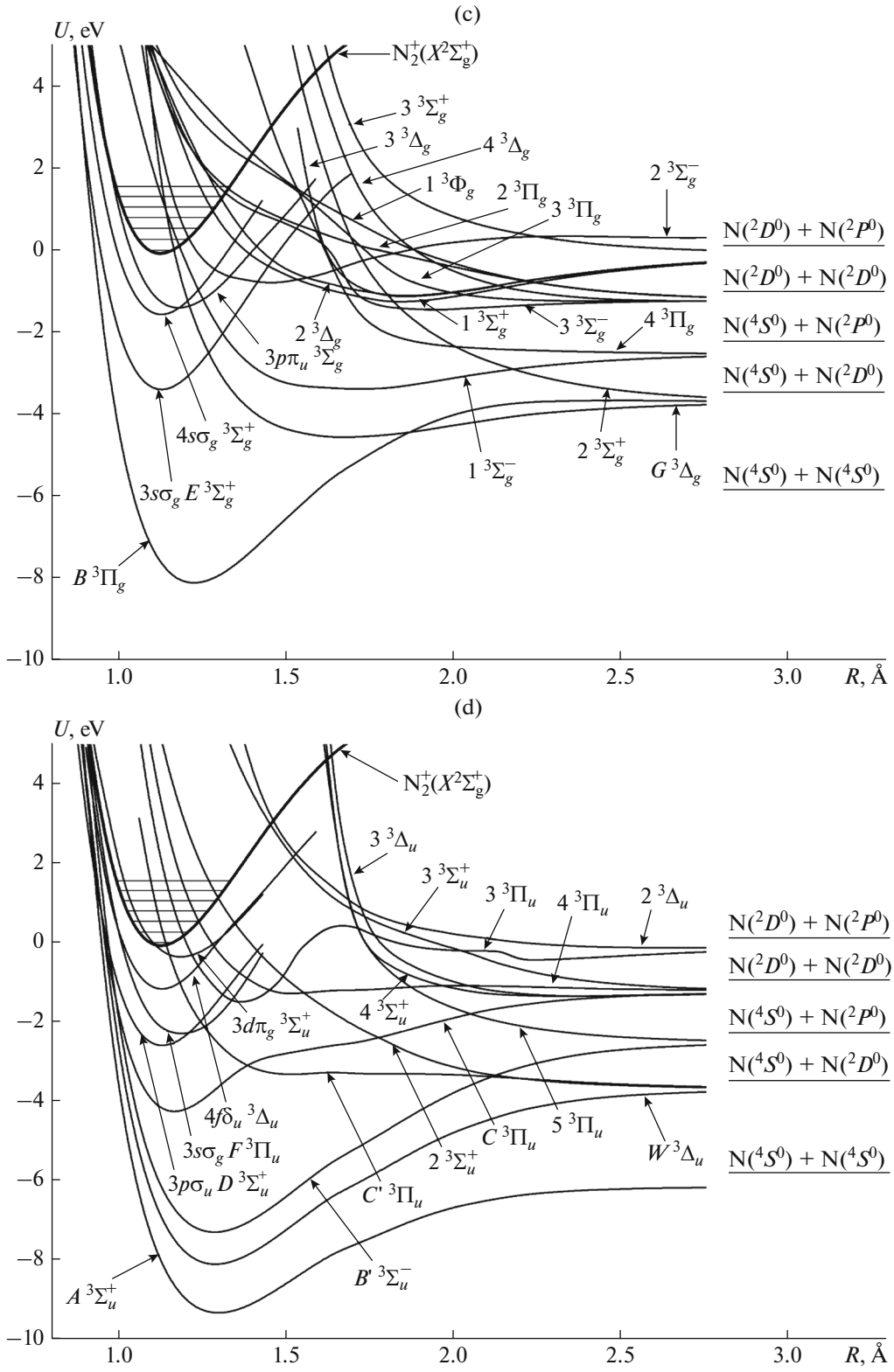
(c)
U, eV
N2+(X2Σg+)
3 3Σg+
3 3Δg
4 3Δg
1 3Φg
2 3Πg
3 3Πg
2 3Σg−
N(2D0) + N(2P0)
N(2D0) + N(2D0)
N(4S0) + N(2P0)
N(4S0) + N(2D0)
N(4S0) + N(4S0)
2 3Δg
3pσu 3Σg+
1 3Σg+
3 3Σg−
4 3Πg
4sσg 3Σg+
3sσg E 3Σg+
1 3Σg−
2 3Σg+
G 3Δg
B 3Πg
R, Å
(d)
U, eV
N2+(X2Σg+)
3 3Δu
3 3Σu+
3 3Πu
4 3Πu
2 3Δu
3dπg 3Σu+
4 3Σu+
4fδu 3Δu
3sσg F 3Πu
3pσu D 3Σu+
2 3Σu+
C 3Πu
5 3Πu
W 3Δu
C' 3Πu
B' 3Σu−
A 3Σu+
R, Å

Fig. 2. (Contd).

Table 2. Values of the adiabatic quantum defects $\mu_{nl\lambda}(R_e)$ for series of Rydberg states of the N_2 molecule

Ionic states	States, Rydberg series $(nl\lambda)$	$\mu_{nl\lambda}(R_e)$*		
		A	B	C
$X^2\Sigma_g^+$	$E^3\Sigma_g^+(3s\sigma_g)$	1.000	1.049	1.070
	$a''^1\Sigma_g^+(3s\sigma_g)$	0.992	0.927	0.940
	$D^3\Sigma_u^+(3p\sigma_u)$	0.826	0.765	0.740
	$c_4'^1\Sigma_u^+(3p\sigma_u)$	0.675	0.725	0.680
	$G^3\Pi_u(3p\pi_u)$	0.673	0.739	0.700
	$c_3^1\Pi_u(3p\pi_u)$	0.642	0.668	0.670
	$d_3^1\Sigma_g^+(3d\sigma_g)$	0.146	0.114	0.150
	$^3\Sigma_g^+(4s\sigma_g)$	0.993	1.155	0.930
	$^3\Pi_g(3d\pi_g)$	–0.020	–0.018	–0.070
	$k^1\Pi_g(3d\pi_g)$	–0.151	–0.047	–0.080
	$c_5'^1\Sigma_u^+(4p\sigma_u)$	0.636	0.694	0.580
$A^2\Pi_u$	$F^3\Pi_u(3s\sigma_g)$	0.978	1.022	1.020
	$o_3^1\Pi_u(3s\sigma_g)$	0.976	0.972	0.980
	$^3\Sigma_g^+(3p\pi_u)$	0.688	0.768	0.670
	$^3\Delta_g(3p\pi_u)$	0.624	0.760	0.710
	$z^1\Delta_g(3p\pi_u)$	0.611	0.704	0.700
	$y^1\Pi_g(3p\sigma_u)$	0.631	0.652	0.600
	$^3\Sigma_g^-(3p\pi_u)$	0.637	0.697	0.760
	$x^1\Sigma_g^-(3p\pi_u)$	0.677	0.696	0.740
	$^3\Delta_u(3d\pi_g)$	–0.016	0.009	–0.080
	$^3\Sigma_u^-(3d\pi_g)$	–0.441	–0.061	–0.060

* A – the results of the present study, B – [11], and C – [13].

whose states converge to the ground state $X^2\Sigma_g^+$ of the N_2^+ ion. The solid lines denote the configuration interactions of the singlet states; the dashed lines denote the same for the triplet ones. It follows from Fig. 3 that the best interacting configurations are the singlet ones of $^1\Sigma_g^+$ and $^1\Pi_u$ symmetry and the triplet ones of $^3\Pi_u$ symmetry.

Figure 4 presents similar results for the matrix elements of interaction $V_{q\beta}^{CI}(R)$ of the dissociative and Rydberg configurations whose states converge to the

Table 3. Diabatic quantum defects and their derivatives for different series of Rydberg states of the N_2 molecule

Ionic states	States, Rydberg series ($nl\lambda$)	$\mu^d_{nl\lambda}(R_e^+)$	$\left.\frac{d\mu^d_{nl\lambda}(R)}{dR}\right\vert_{R_e^+}$
$X^2\Sigma_g^+$	$E^3\Sigma_g^+(3s\sigma_g)$	0.970	0.023
	$a''^1\Sigma_g^+(3s\sigma_g)$	0.905	0.050
	$D^3\Sigma_u^+(3p\sigma_u)$	0.730	−0.203
	$c_4'^1\Sigma_u^+(3p\sigma_u)$	0.725	0.100
	$G^3\Pi_u(3p\pi_u)$	0.639	0.428
	$c_3{}^1\Pi_u(3p\pi_u)$	0.632	0.563
	$d_3{}^1\Sigma_g^+(3d\sigma_g)$	0.061	−0.039
	$^3\Sigma_g^+(4s\sigma_g)$	1.008	−0.073
	$^3\Pi_g(3d\pi_g)$	0.159	0.507
	$k^1\Pi_g(3d\pi_g)$	0.184	−0.135
	$c_5'^1\Sigma_u^+(4p\sigma_u)$	0.552	0.205
$A^2\Pi_u$	$F^3\Pi_u(3s\sigma_g)$	0.979	0.029
	$o_3{}^1\Pi_u(3s\sigma_g)$	1.009	−0.023
	$^3\Sigma_g^+(3p\pi_u)$	0.685	0.124
	$^3\Delta_g(3p\pi_u)$	0.721	−0.184
	$z^1\Delta_g(3p\pi_u)$	0.609	−0.094
	$y^1\Pi_g(3p\sigma_u)$	0.622	−0.080
	$^3\Sigma_g^-(3p\pi_u)$	0.653	0.120
	$x^1\Sigma_g^-(3p\pi_u)$	0.599	−0.090
	$^3\Delta_u(3d\pi_g)$	0.130	0.205
	$^3\Sigma_u^-(3d\pi_g)$	−0.062	0.000

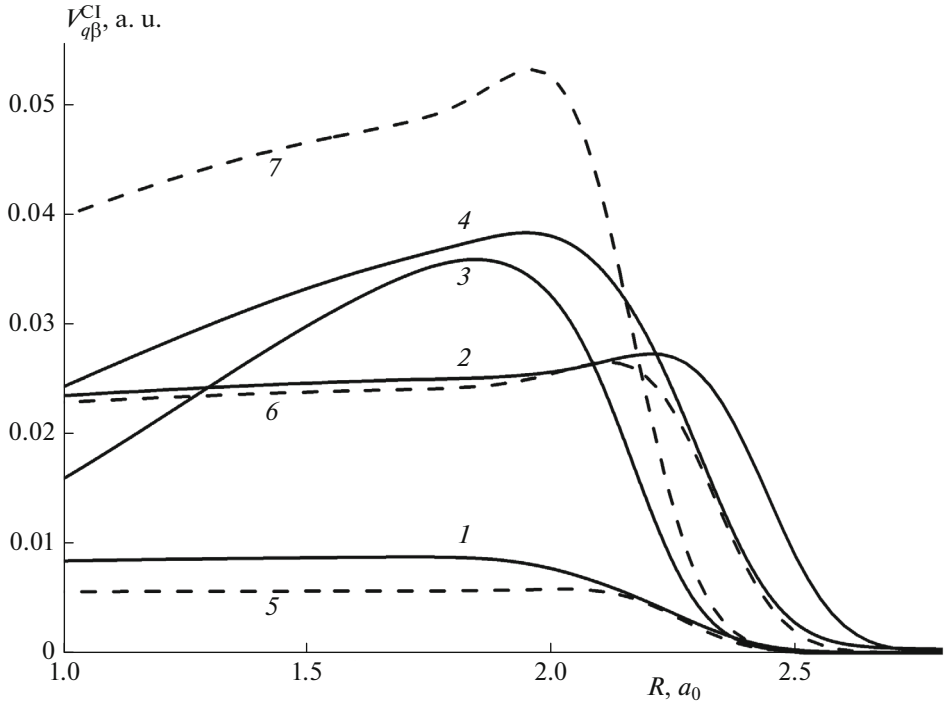

Fig. 3. Matrix elements of interaction $V_{q\beta}^{CI}(R)$ of the dissociative and Rydberg configurations whose states converge to the ground state $X^2\Sigma_g^+$ of the N_2^+ ion: (*1*) $V_{q\beta}^{CI}(f\varphi_u - {}^1\Phi_u)$, (*2*) $V_{q\beta}^{CI}(p\pi_u - 3^1\Pi_u)$, (*3*) $V_{q\beta}^{CI}(s\sigma_g - a''^1\Sigma_g^+)$, (*4*) $V_{q\beta}^{CI}(p\pi_u - 2^1\Pi_u)$, (*5*) $V_{q\beta}^{CI}(p\pi_u - 3^3\Pi_u)$, (*6*) $V_{q\beta}^{CI}(p\pi_u - 4^3\Pi_u)$, and (*7*) $V_{q\beta}^{CI}(p\pi_u - 2^3\Pi_u)$.

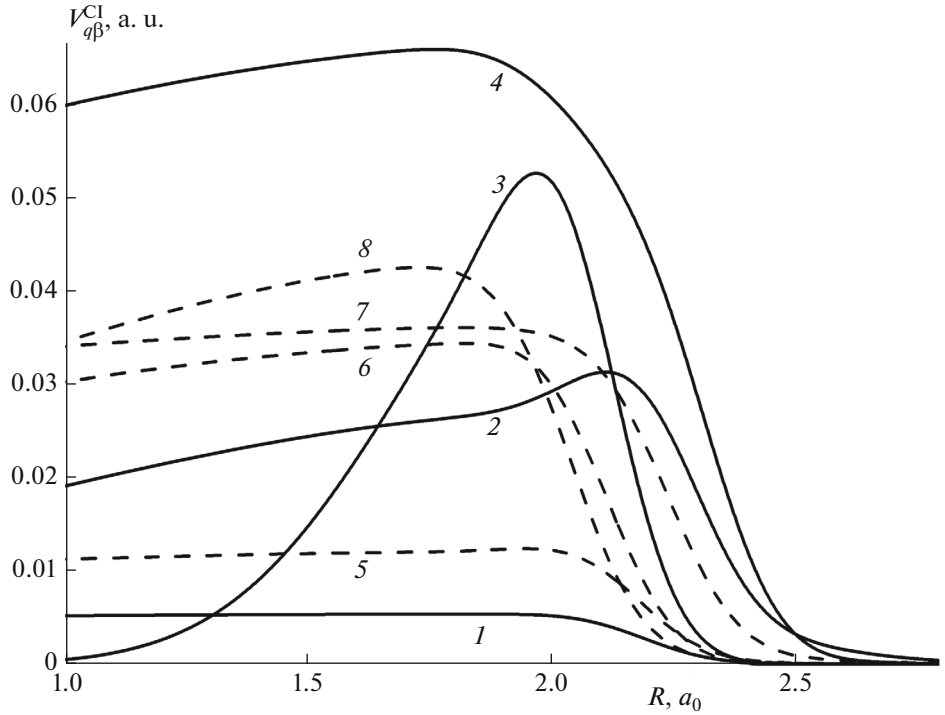

Fig. 4. Matrix elements of interaction of the dissociative and Rydberg configurations whose states converge to the first electron-excited state $A^2\Pi_u$ of the N_2^+ ion: (*1*) $V_{q\beta}^{CI}(s\sigma_g - 3^1\Pi_u)$, (*2*) $V_{q\beta}^{CI}(s\sigma_g - 2^1\Pi_u)$, (*3*) $V_{q\beta}^{CI}(p\pi_u - a''^1\Sigma_g^+)$, (*4*) $V_{q\beta}^{CI}(p\pi_u - 1^1\Delta_g)$, (*5*) $V_{q\beta}^{CI}(s\sigma_g - 3^3\Pi_u)$, (*6*) $V_{q\beta}^{CI}(p\pi_u - G^3\Delta_g)$, (*7*) $V_{q\beta}^{CI}(s\sigma_g - 4^3\Pi_u)$, and (*8*) $V_{q\beta}^{CI}(s\sigma_g - C'^3\Pi_u)$.

first electronically excited $A^2\Pi_u$ state of the N_2^+ ion. Here we can state that the best interacting configurations are the singlet ones of $^1\Sigma_g^+$, $^1\Pi_u$, and $^1\Delta_g$ symmetry and the triplet ones of $^3\Pi_u$ and $^3\Delta_g$ symmetry.

4. CONCLUSIONS

The adiabatic potential curves were calculated by the CMRCI method for 20 valence and 22 Rydberg singlet and triplet configurations of the nitrogen molecule. The detailed comparison of the obtained data with experiment and other calculations convincingly showed high accuracy of the present results.

As a result of the use of the diabatization method, a picture of diabatic terms was constructed, and the diabatic quantum defects and radial matrix elements of the configuration interaction of dissociative and Rydberg configurations whose states converge to the ground state $X^2\Sigma_g^+$ and the first electronically excited ion state $A^2\Pi_u$ were calculated. These data will be used to calculate the partial and total cross sections and rate constants of DR and AI within the framework of the integral variant of the MQD theory. In this case, it suffices to include only the singlet configurations related to $^1\Sigma_g^+$, $^1\Pi_u$, and $^1\Delta_g$ symmetry and the triplet ones related to $^3\Pi_u$ and $^3\Delta_g$ symmetry. The contribution of the remaining states will be negligibly small.

Recently, theoretical studies have been actively conducted to investigate the optical quantum properties of the D and E layers of the Earth's ionosphere, which arise during the periods of strong geomagnetic disturbances of the ionosphere due to high solar activity [19]. The positioning errors of the global navigation satellite systems (GNSSs) generally increase in these periods. At stronger geomagnetic disturbances, the signal on the GNSS receiver can completely disappear and does not appear for a long time [20]. The uncontrolled sporadic violations of satellite signals are due to phase and group delays during the propagation of electromagnetic radiation [21].

It was found that during the periods of high solar activity, the Rydberg molecular complexes responsible for the distortion of the satellite signals are populated in the D and E layers of the ionosphere [22]. The radiative transitions between the orbitally degenerate states of these complexes form incoherent additional background radiation in the decimeter (microwave) and terahertz (IR) bands. Therefore, today construction of the potential energy surfaces of the Rydberg states of the nitrogen and oxygen molecules perturbed by the neutral molecules of the gaseous medium is a challenge.

ACKNOWLEDGMENTS

The present study was performed within the framework of the State Assignment of Russian Federal Agency of Scientific Organizations (project 0082-2018-0001, registration code AAAA-A17-117112240026-5).

REFERENCES

1. S. L. Guberman, J. Chem. Phys. **137**, 074309 (2012).
2. D. A. Little and J. Tennyson, J. Phys. B **46**, 145102 (2013).
3. K. P. Huber and G. Herzberg, *Constants of Diatomic Molecules* (Van Nostrand-Reinhold, New York, 1979).
4. H. J. Werner, P. J. Knowles, G. Knizia, et al., MOLPRO, Vers. 2010.1, A Package of ab initio Programs. http://www.molpro.net.
5. P. O. Widmark, P. A. Malmqvist, and B. O. Roos, Theor. Chim. Acta **77**, 291 (1990).
6. M. G. Golubkov, G. K. Ozerov, S. O. Adamson, et al., Chem. Phys. **462**, 28 (2015).
7. M. Hochlaf, H. Ndome, D. Hammoutene, et al., J. Phys. B: At., Mol. Opt. Phys. **43**, 245101 (2010).
8. A. Lofthus and P. H. Krupenie, J. Phys. Chem. Ref. Data **6**, 113 (1977).
9. K. P. Huber and Ch. Jungen, J. Chem. Phys. **92**, 850 (1990).
10. D. Cossart and C. Cossart-Magos, J. Chem. Phys. **121**, 7148 (2004).
11. B. R. Lewis, A. N. Heays, S. T. Gibson, et al., J. Chem. Phys. **129**, 164306 (2008).
12. H. H. Michels, J. Chem. Phys. **53**, 841 (1970).
13. P. Cremaschi, A. Chattopadhyay, P. V. Madhavan, et al., Chem. Phys. **109**, 117 (1986).
14. G. V. Golubkov, M. G. Golubkov, and A. N. Romanov, J. Exp. Theor. Phys. **94**, 489 (2002).
15. G. V. Golubkov, M. G. Golubkov, A. N. Romanov, et al., Phys. Chem. Chem. Phys. **5**, 3174 (2003).
16. G. V. Golubkov, M. G. Golubkov, and R. J. Buenker, J. Exp. Theor. Phys. **112**, 187 (2011).
17. G. K. Ozerov, M. G. Golubkov, G. V. Golubkov, et al., High Energy Chem. **50**, 85 (2016).
18. S. O. Adamson, R. J. Buenker, G. V. Golubkov, et al., Russ. J. Phys. Chem. B **3**, 195 (2009).
19. G. V. Golubkov, M. I. Manzhelii, A. A. Berlin, et al., Russ. J. Phys. Chem. B **10**, 77 (2016).
20. G. V. Golubkov, M. G. Golubkov, and M. I. Manzhelii, Dokl. Phys. **57**, 461 (2012).
21. G. V. Golubkov, M. G. Golubkov, and M. I. Manzhelii, Dokl. Phys. **58**, 424 (2013).
22. G. V. Golubkov, M. G. Golubkov, and M. I. Manzhelii, Russ. J. Phys. Chem. B **6**, 112 (2012).

Translated by L. Smolina